

Multi Focus Image Fusion using Logarithmic NSCT

Bhavana S G¹, Swati Kalaskar²

¹Assistant Professor, Dept of CSE, VTU PG Center & Regional Office, Gulbarga, India

²Dept of CSE, VTU PG Center & Regional Office, Gulbarga, India

Abstract- Image fusion is used to integrate complementary information from many images to create a more highly informative image which is suitable for human visual system and computer processing tasks. In multi-focus image fusion, the images that have different focus areas are merged to produce the all in focus image. This paper includes the problems of both transform domain-based spatial domain-based image fusion. First the source image is decomposed using logarithmic NSCT. Now low frequency sub-band coefficients are fused using sum-modified Laplacian-based local visual contrast and high frequency sub band coefficients are fused using local Log-Gabor energy. The final fused image is subsequently reconstructed based on the inverse logarithmic NSCT with the fused coefficients. Experimental results shows that the proposed method is better than existing fusion methods including gradient pyramid transform, discrete wavelet transform and NSCT.

Key Words - Multi-focus image fusion, Non sub-sampled Contourlet transform, Log-Gabor energy

1. INTRODUCTION

Image fusion can be defined as a process in which a new image is produced by integrating complementary, multi-temporal or multi-view information from a set of source images. The resultant image acquired from image fusion technique is more informative and appropriate for the purposes of human visual perception and further image processing tasks such as segmentation, feature extraction and target recognition. Multi-focus image fusion is an important branch of this field. Due to the limited depth-of-focus of optical lenses in camera, it is often not possible to obtain an image that contains all relevant focused objects. One way to overcome this problem is by using the multi-focus image fusion technique, through which several images with different focus points are combined to form a single image with all objects fully focused. Image fusion methods are usually divided into spatial domain and transform domain fusion techniques. Fusion methods in the spatial domain are directly on pixel gray level or color

space from the source images for fusion operation, so the spatial domain fusion methods are also known as single-scale fusion method. For transform domain-based methods, each source image is first decomposed into a sequence of images through a particular mathematical transformation. Then, the fused coefficients are obtained through some fusion rules for combination. Finally, the fusion image is obtained by means of a mathematical inverse transform. Recently, the more popular fusion methods using Multi-scale Transform (MST) have been explored, including the Laplacian Pyramid Transform, Gradient Pyramid Transform (GP), Wavelet Transform, Log-Gabor Transform and other MST. To overcome these shortcomings of the wavelet transform, M. N. Do and M. Vetterli proposed the Contourlet Transform (CT), which can give the asymptotic optimal representation of contours and has been successfully used for image fusion. However, the up- and down-sampling process of Contourlet decomposition and reconstruction results in the CT lacking shift-invariance and having pseudo-Gibbs phenomena in the fused image. On the foundation of CT, A. L. Cunha et al. proposed the Non-subsampled Contourlet Transform (NSCT). NSCT inherits the advantages of CT, while also possessing shift-invariance and effectively suppressing Pseudo-Gibbs phenomena. Thus, the NSCT is more suitable for image fusion. In addition, it is noteworthy that most of the image fusion methods are based on the assumption that the source images are noise-free, and they can produce high-quality fused images in the hypothesis. However, practically, the images are often corrupted by noise during the processes of image acquisition. Based on the above analysis, an image fusion method based on logarithmic NSCT and focused area detection is proposed in this paper.

2. RELATED WORK

This section provides the related concepts on which the proposed framework is based. These concepts, including NSCT and NSCT for image fusion, are described as follows.

2.1 Non-Subsampled Contourlet Transform

CT can be divided into two stages, including the Laplacian Pyramid (LP) and Directional Filter Bank (DFB), and offers an efficient directional multi-resolution image representation. Among them, LP is first used to capture the point singularities, and then followed by DFB to link the singular point into linear structures. LP is employed to decompose the original images into low frequency and high frequency sub-images, and then the DFB divides the high frequency subbands into directional subbands. A contourlet decomposed schematic diagram is shown in Fig. 1.

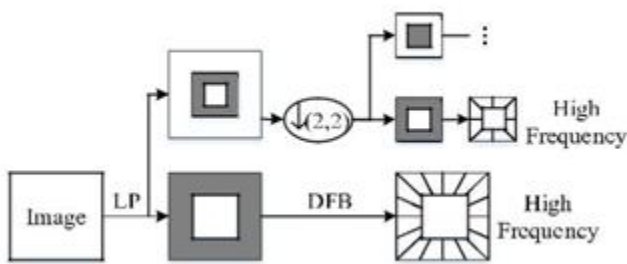


Fig -1 Schematic diagram of Contourlet Transform

During the realization of the CT, the decomposition and construction filters of LP are separable bi-orthogonal filters with bandwidth greater than $\pi/2$. According to the sampling theorem, the pseudo-Gibbs phenomena would appear in low- and high-frequency sub-images in LP domain. Directional subbands which come from the high frequency sub-images by DFB filtering would also appear the pseudo- Gibbs phenomena. These phenomena would weaken the directional selectivity of the CT based method to some extent. To solve this problem, A. L. Cunha et al. proposed NSCT based on the theory of CT. NSCT inherits the advantage of CT, enhances directional selectivity and shift-invariance, and effectively overcomes the pseudo-Gibbs phenomena. NSCT is based on Non-subsampled Pyramid Filter Banks (NSPFB) and Non-subsampled Directional Filter Banks (NSDFB).

2.2 NSCT-Based Image Fusion

In this subsection, the NSCT-based image fusion scheme, which is used in this paper, will be discussed. Considering a pair of input images, A and B, the NSCT-based image fusion can be described by the following steps:

Step 1: Perform θ -level NSCT on images A and B to obtain one low frequency subband and a series of high frequency subbands at each level and direction l , i.e., A: L_A, H_{Akl} and B: L_B, H_{Bkl} , where L_A, L_B are the low frequency sub-images and H_{Akl}, H_{Bkl} represent the high frequency sub-images at level $k \in [1, \theta]$ in the orientation l .

Step 2: Fuse low frequency subbands and high frequency subbands through certain fusion rules to obtain fused low frequency (LF) and high frequency (HF kl) subbands.

Step 3: Perform θ -level inverse NSCT on the fused low frequency subband and high frequency subbands to obtain the fused image. The framework of NSCT-based image fusion methods is shown in Fig. 3.

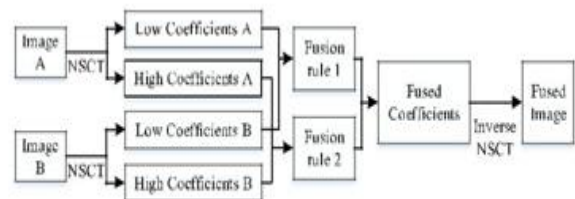


Fig -2 NSCT based fusion algorithm diagram

3. FUSED IMAGE BASED ON LOGARITHMIC NSCT

Due to the beneficial properties of NSCT for image fusion, we choose NSCT decomposition and reconstruction to obtain the fused image.

3.1 Fusion of Low Frequency Subbands

The coefficients in the low frequency subbands, representing the approximate information of source images, reflect the gray component of source images and contain the most energy of source images. For spatial-based multi-focus image fusion, many typical focus measurements, such as energy of image gradient, Spatial Frequency, Tenengrad, laplacian energy and SML, are compared. SML proves itself to be the best measurement [30]. In the transform domain, SML is also very efficient and can produce the best fused result [31]. SML is defined as:

$$SML(i, j) = \sum_{m=-M}^M \sum_{n=-N}^N [ML(i+m, j+n)] \dots\dots (1)$$

for a window with size $(2M + 1)(2N + 1)$, where $ML(i, j)$ is the Modified Laplacian (ML), which is defined as:

$$ML(i, j) = |2L(i, j) - L(i - step, j) - L(i + step, j)| + |2L(i, j) - L(i, j - step) - L(i, j + step)| \dots\dots\dots (2)$$

where step is a variable spacing between coefficients and always is equal to 1 [30]. $L(i, j)$ denotes the coefficient located at (i, j) in low frequency subbands. According to physiological and psychological research, HVS is highly sensitive to the local image contrast rather than the pixel value itself. To meet this requirement, local visual contrast is proposed. Considering the local visual contrast and excellent clear measurement of SML, the fusion rule of low frequency coefficients presented in this article employs SML based local visual contrast. This scheme is defined as:

$$LV(i, j) = \begin{cases} SML(i, j) \wedge L(i, j) \cdot 1 + \alpha, & \text{if } L(i, j) = 0 \\ SML(i, j), & \text{otherwise} \end{cases} \dots\dots\dots (3)$$

where $\alpha \in (0.6, 0.7)$ is a visual constant that is the slope of the best-fitted lines by means of high-contrast data. The low frequency subbands are fused as:

$$LF(i, j) = \begin{cases} LA(i, j), & \text{if } LVA(i, j) \geq LVB(i, j) \\ LB(i, j), & \text{otherwise} \end{cases} \dots\dots (4)$$

where $LF(i, j)$ represents the coefficient located at (i, j) in low frequency subbands of the initial fused image.

3.2 Fusion of High Frequency Subbands

The high frequency coefficient subbands represent the detailed components of the source images, such as the edges, textures, boundaries, and so on. Generally, the coefficients with larger absolute values are considered as the coefficients with more clearly detailed features or sharp brightness changes, but it is noteworthy that the

noise is also related to high frequencies and may cause miscalculation of sharpness values and, therefore, affect the fusion performance. Thus, for the high frequency coefficients, the most common fusion rule is to select coefficient with larger absolute values. However, this scheme does not take any consideration of the surrounding pixels. The value of a single pixel of high frequency coefficients is used to contrast the measurement of the high frequency component. This is especially true when the input contains noise, as the noise can be mistaken for fused coefficients and cause miscalculation of the sharpness value. Furthermore, humans are often sensitive to texture detail features, but are insensitive to the value of a single pixel.

To overcome the defect mentioned above, inspired by the literature and combining the concept of local energy, a new high frequency fusion rule based on local Log-Gabor energy is designed in this article. Gabor filters is a popular technique that has been extensively used to extract texture features. Log-Gabor filters are proposed based on Gabor filters. Compared with Gabor filters, Log-Gabor filters, whose transfer function covers the shortage of the high frequency of Gabor filter component expression, are more in accord with HVS. Therefore, Log-Gabor filters can achieve optimal spatial orientation and wider spectrum information at the same time and thus more truly reflect the frequency response of the natural images and improve performance in terms of the accuracy. Under polar coordinates, the Log-Gabor filter is defined as follows:

$$g(f, \theta) = \exp \left\{ - \frac{[\ln(\frac{f}{f_0})]^2}{2[\ln(\frac{\sigma}{f_0})]^2} \right\} \times \exp \{ -(\theta - \theta_0)^2 / 2\sigma^2 \} \dots\dots\dots (5)$$

in which f_0 is the center frequency of the Log-Gabor filter, θ_0 is the direction of the filter, σ is used to determine the bandwidth, B_f , of the radial filter, and $\sigma\theta$ is used to determine the bandwidth, B_θ , of the orientation.

4. THE FRAMEWORK OF THE PROPOSED IMAGE FUSION METHOD

Combining the advantages of the transform domain method and spatial domain method, a novel algorithm

based on NSCT and focused area detection is proposed. The schematic diagram of the algorithm is illustrated in Fig. 3

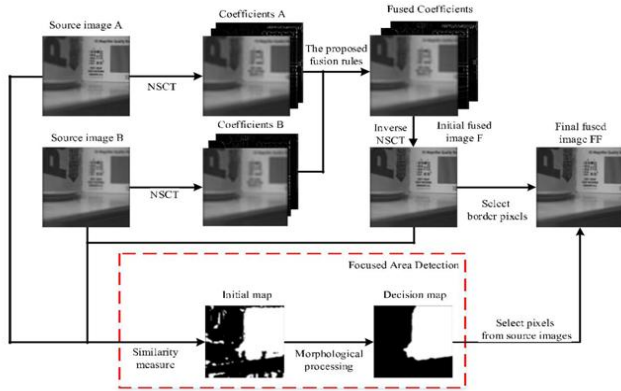


Fig- 3 Block Diagram of Proposed Image Fusion

The proposed scheme can be presented as the following steps:

Step 1: Use the NSCT-based fusion method through a novel couple of fusion rules described in Section 3 to obtain the initial fused image, F.

Step 2: After obtaining the initial fusion image, RMSE is applied to measure the similarity between each input image and the initial fused image F. The focused area detection method is utilized to calculate the focus area and obtain the decision map $Z(i, j)$ of the source images.

Step 3: Use the decision map $Z(i, j)$ to guide the final fusion processing and achieve the final fusion image, FF. This process can be illustrated as the following:

$$FF(i, j) = \begin{cases} A(i, j), & \text{if } T(i, j) = (2M + 1)(2N + 1) \\ B(i, j), & \text{if } T(i, j) = 0 \\ F(i, j), & \text{otherwise} \end{cases} \quad \dots\dots(6)$$

$$T(i, j) = \sum_{m=-M}^M \sum_{n=-N}^N Z(i, j) \quad \dots\dots\dots (7)$$

where $T(i, j)$ is the sum values of decision map $Z(i, j)$ at the local area around the pixel (i, j) . $F(i, j)$ and $FF(i, j)$ are the values of the pixel located at the coordinates (i, j) of the initial fused image and the final fused image, respectively. $(2M + 1)(2N + 1)$ is the size of the window, and the value of $T(i, j)$ can be used to judge whether the pixel is at the edge area between the area in focus and the area out of focus.

In equation (21), $T(i, j) = (2M + 1)(2N + 1)$ shows that, in the decision map, the pixels around the pixel at (i, j) are all 1, which suggests that the pixel at (i, j) in source A is in the focused area and can be selected as the pixel of the final fused image, directly.

Alternately, $T(i, j) = 0$ indicates that the corresponding pixel (i, j) from source B is located in the focused area and can be selected as the pixel of the final fused image.

Otherwise, $0 < T(i, j) < (2M + 1)(2N + 1)$ means that the pixels located at (i, j) is in the focused border area. To avoid the fused image discontinuous, the pixels of the final fused image in this area were selected from the initial fused image.

5. EXPERIMENTAL RESULT SETS

5.1 Evaluation Index System

Some general requirements for a good image fusion scheme are: (1) it should be able to extract the complementarily information from source images; (2) it should be robust and reliable; and (3) it must not introduce inconsistencies or artifacts according to HVS

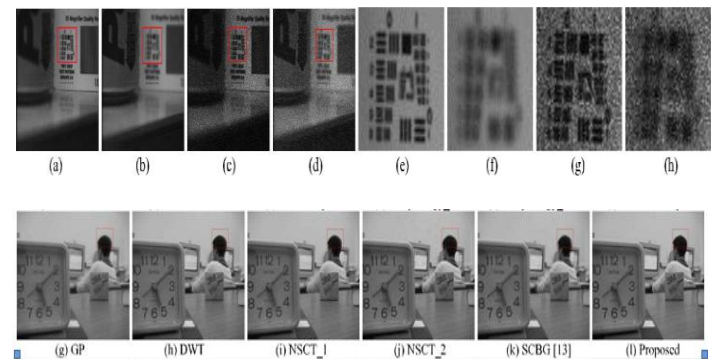


Fig- 4 The Experimental data and results of fusing mis-registration multi-focus images

The main objective of this evaluations are easily performed by computers, completely automatically which can be generally evaluate the similarity between fused images and source image. Therefore, besides visual observations, five objective criteria are used to evaluate the proposed fusion scheme.

- Mutual Information : It indicates how much information the fused image conveys about the two source images. Therefore, the greater value of mutual information, the better the fusion effect.

- Edge-Dependent Fusion Quality Index : Edge-dependent fusion quality index (QE) assesses the pixel-level fusion performance objectively. The larger the Quality Index value , the better the fused result.
- Edge Based Similarity Measure : The edge-based similarity measure (QAB/F) gives the similarity between the edges transferred from the input images to the fused image. Therefore, the larger the value, the better the fusion effect result.
- Structural Similarity-Based Metric : Structural similarity (SSIM) is designed by modeling any image distortion as the combination of the loss of correlation and radiometric and contrast distortion. SSIM reflects the structural similarity between the standard reference image and the fused image. The larger the value the better the fusion effect.

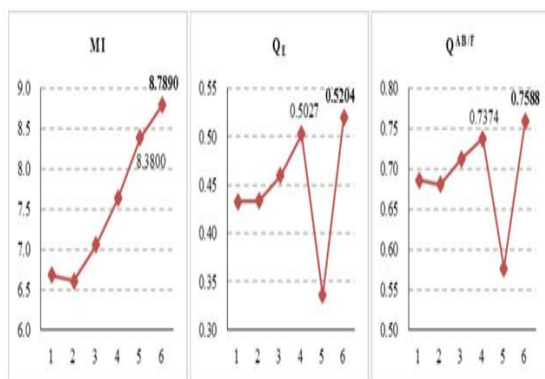


Chart 1- Comparison on objective criteria of fusing mis-registration multi-focus images.

Images	Evaluation	GP	DWT	NSCT_1	NSCT_2	SCBG [13]	Proposed method
Pepsi	MI	6.5204	6.6331	7.2363	8.1904	8.6527	9.1805
	Qi	0.5534	0.5542	0.5805	0.6542	0.4617	0.6707
	QAB/F	0.6895	0.6837	0.7107	0.7366	0.6258	0.7588
Clock	MI	6.3777	6.5325	6.8946	7.7230	8.4652	8.6580
	Qi	0.4753	0.4981	0.5027	0.5643	0.4087	0.5823
	QAB/F	0.6878	0.6786	0.7092	0.7258	0.5946	0.7502

Table 1-Comparisson between Different Methods and Multi Focus Image

- Correlation Coefficient : Correlation coefficient (CORR) between the standard reference image and the fused image is defined as the average pixel vales of the standard reference image and the fused image , respectively. This quality

reflects the degree of correlation between the standard reference image and fused image. The larger the value, the better the fusion effect.

6. CONCLUSION

In this paper, image fusion scheme that is based on logarithmic NSCT and focused area detection is proposed for multi-focus image fusion. NSCT is more suitable for image fusion because of superiorities such as multi-resolution, multi-direction, and shift-invariance. The proposed fusion scheme can prevent artifacts and erroneous results at the boundary of the focused areas that may be introduced by detection focused area based methods during the fusion process. The experimental results on several groups of multi-focus images, regardless of whether there is noise or not, have shown the superior performance of the proposed fusion scheme.

REFERENCES

[1] Y. Jiang and M. Wang, "Image fusion with morphological component analysis," *Inf. Fusion*, vol. 18, no. 1, pp. 107–118, Jul. 2014.

[2] S. Li and B. Yang, "Hybrid multiresolution method for multisensor multimodal image fusion," *IEEE Sensors J.*, vol. 10, no. 9, pp. 1519–1526, Sep. 2010.

[3] S. Chen, R. Zhang, H. Su, J. Tian, and J. Xia, "SAR and multispectral image fusion using generalized IHS transform based on à trous wavelet and EMD decompositions," *IEEE Sensors J.*, vol. 10, no. 3, pp. 737–745, Mar. 2010.

[4] B. Miles, I. B. Ayed, M. W. K. Law, G. Garvin, A. Fenster, and S. Li, "Spine image fusion via graph cuts," *IEEE Trans. Biomed. Eng.*, vol. 60, no. 7, pp. 1841–1850, Jul. 2013.

[5] J. Liang, Y. He, D. Liu, and X. Zeng, "Image fusion using higher order singular value

decomposition," *IEEE Trans. Image Process.*, vol. 21, no. 5, pp. 2898–2909, May 2012.

[6] B. Yang and S. Li, "Multi-focus image fusion using watershed transform and morphological wavelet clarity measure," *Int. J. Innovative Comput. Inf. Control.*, vol. 7, no. 5A, pp. 2503–2514, May 2011.

[7] B. Yang and S. Li, "Multifocus image fusion and restoration with sparse representation," *IEEE Trans. Instrum. Meas.*, vol. 59, no. 4, pp. 884–892, Apr. 2010.

[8] W. Wang and F. Chang, "A multi-focus image fusion method based on Laplacian pyramid," *J. Comput.*, vol. 6, no. 12, pp. 2559–2566, Dec. 2011.

[9] N. Mitianoudis and T. Stathaki, "Optimal contrast correction for ICA-based fusion of multimodal images," *IEEE Sensors J.*, vol. 8, no. 12, pp. 2016–2026, Dec. 2008.

[10] V. Aslantas and R. Kurban, "Fusion of multi-focus images using differential evolution algorithm," *Expert Syst. Appl.*, vol. 37, no. 12, pp. 8861–8870, Dec. 2010.

[11] I. De and B. Chanda, "Multi-focus image fusion using a morphologybased focus measure in a quad-tree structure," *Inf. Fusion*, vol. 14, no. 2, pp. 136–146, Apr. 2013.

[12] S. Li, J. T. Kwok, and Y. Wang, "Multifocus image fusion using artificial neural networks," *Pattern Recognit. Lett.*, vol. 23, no. 8, pp. 985–997, Jun. 2002.

[13] J. Tian, L. Chen, L. Ma, and W. Yu, "Multi-focus image fusion using a bilateral gradient-based sharpness criterion," *Opt. Commun.*, vol. 284, no. 1, pp. 80–87, Jan. 2011.

[14] G. Piella, "A general framework for multiresolution image fusion: From pixels to regions," *Inf. Fusion*, vol. 4, no. 4, pp. 259–280, Dec. 2003.

[15] S. Li, X. Kang, J. Hu, and B. Yang, "Image matting for fusion of multi-focus images in dynamic scenes," *Inf. Fusion*, vol. 14, no. 2, pp. 147–162, Apr. 2013.

[16] Y. Liu, J. Jin, Q. Wang, Y. Shen, and X. Dong, "Region level based multi-focus image fusion using quaternion wavelet and normalized cut," *Signal Process.*, vol. 97, pp. 9–30, Apr. 2014.

[17] B. Aiazzi, L. Alparone, A. Barducci, S. Baronti, and I. Pippi, "Multispectral fusion of multisensor image data by the generalized Laplacian pyramid," in *Proc. IEEE Int. Geosci. Remote Sens. Symp.*, Hamburg, Germany, Jun. 1999, pp. 1183–1185.

[18] V. S. Petrovic and C. S. Xydeas, "Gradient-based multiresolution image fusion," *IEEE Trans. Image Process.*, vol. 13, no. 2, pp. 228–237, Feb. 2004.

[19] Y. Yang, S. Y. Huang, J. Gao, and Z. Qian, "Multi-focus image fusion using an effective discrete wavelet transform based algorithm," *Meas. Sci. Rev.*, vol. 14, no. 2, pp. 102–108, Apr. 2014.

[20] H. Li, B. S. Manjunath, and S. K. Mitra, "Multisensor image fusion using the wavelet transform," *Graph. Models Image Process.*, vol. 57, no. 3, pp. 235–245, May 1995.

[21] K. Kannan, S. A. Perumal, and K. Arulmozhi, "Area level fusion of multi-focused images using multi-stationary wavelet packet transform," *Int. J. Comput. Appl.*, vol. 2, no. 1, pp. 88–95, 2010.

[22] S. Li, J. T. Kwok, and Y. Wang, "Using the discrete wavelet frame transform to merge Landsat TM and SPOT panchromatic images," *Inf. Fusion*, vol. 3, no. 1, pp. 17–23, Mar. 2002.

[23] Z. Zhou, S. Li, and B. Wang, "Multi-scale weighted gradient-based fusion for multi-focus images," *Inf. Fusion*, vol. 20, pp. 60–67, Nov. 2014.

[24] M. N. Do and M. Vetterli, "The contourlet transform: An efficient directional multiresolution image representation," *IEEE Trans. Image Process.*, vol. 14, no. 12, pp. 2091–2106, Dec. 2005.

[25] X. B. Qu, J. W. Yan, and G. D. Yang, "Multi-focus image fusion method of sharp frequency localized contourlet transform domain based on

summodified-Laplacian," *Opt. Precis. Eng.*, vol. 17, no. 5, pp. 1203–1211, May 2009.

[26] A. L. da Cunha, J. Zhou, and M. N. Do, "The nonsubsampling contourlet transform: Theory, design, and applications," *IEEE Trans. Image Process.*, vol. 15, no. 10, pp. 3089–3101, Oct. 2006.

[27] G. Bhatnagar, Q. M. J. Wu, and Z. Liu, "Directive contrast based multimodal medical image fusion in NSCT domain," *IEEE Trans. Multimedia*, vol. 15, no. 5, pp. 1014–1024, Aug. 2013.

BIBLIOGRAPHY



Swati Kalaskar is currently perceiving M.Tech degree in Visveswarayya Technological University PG Center and RO Gulbarga. She has perceived her Bachelor of Engineering in PDA College Engineering Gulbarga Karnataka, India.

Her current research interest includes Image Fusion and Digital Image Processing.